PHYSICAL REVIEW A VOLUME 16, NUMBER 2 AUGUST 1977

Energy and angular distribution of electrons ejected from argon by 5-keV to 1.5-MeV protons*

T. L. Criswell and L. H. Toburen
Battelle Memorial Institute, Pacific Northwest Laboratories, Richland, Washington 99352

M. E. Rudd
Behlen Laboratory of Physics, University of Nebraska, Lincoln, Nebraska 68508
(Received 22 February 1977)

Cross sections, differential in emission energy and angle, have been measured for the ejection of electrons in collisions of H^+ with argon gas targets. Incident-proton energies studied were from 5 keV to 1.5 MeV and electron emission angles ranged from 10° to 160°. Integration of the double-differential cross sections over emission angle and energy yield results in good agreement with direct measurement of total ionization cross sections. The electron distributions are compared to two plane-wave Born-approximation calculations, one using Hartree-Slater wave functions and the other using Hartree-Fock wave functions in the $3p$-ϵd channel.

INTRODUCTION

In a recent study by Manson and Toburen,[1] experimental and theoretical cross sections differential in electron energy and ejection angle were compared for 1-MeV proton impact on argon. A plane-wave Born approximation (PWBA) calculation, using discrete and continuum Hartree-Fock wave functions for the $3p$-ϵd channel and Hartree-Slater wave functions for the remaining channels, was used to calculate the electron distributions. Theory and experiment were found to be in excellent agreement for distributions in both electron energy ϵ and ejection angle θ above ejected electron energies of approximately 65 eV. Discrepancies for lower electron energies are understood in terms of the inability of the calculation to accurately predict the position of the Cooper minimum.[2,3] Further, charge exchange to the continuum, which is a large effect in proton-helium collisions,[4] was found to be a small effect in the proton-argon case. The present study was undertaken to extend this comparison over a broad proton-energy range, particularly to very low proton energies, in order to identify regions where this PWBA calculation is reliable.

Previously published measurements[5] of the energy and angular distribution of electrons ejected from argon have covered the proton energies from 50 to 300 keV, and recently Gabler has measured similar cross sections at 300 to 500 keV and 4.2 to 5.0 MeV.[6] In these works, it was found that the cross sections increased with decreasing proton energy E_p, down to 50 keV. The angular distributions became more forward peaked for lower proton energies, but with additional peaking in the backward directions. In a later study,[7] the cross sections and anisotropy were found to decrease with decreasing proton energy below 50 keV.

The present study presents data on proton impact on argon from 5 keV to 1.5 MeV. The resulting absolute electron-ejection cross sections differential in electron energy and ejection angle are compared to previous experiments and to the PWBA calculations by Manson[3] and Madison.[8] The importance of the $3p$-ϵd channel is noted, and the accuracy of the existing PWBA calculations at low energies is tested.

EXPERIMENTAL PROCEDURE

This experiment consists of measuring the yield of electrons ejected in collisions between a proton beam and a gas target and converting the yield to absolute cross sections. Four sets of apparatus were used in order to cover the ranges of the scattering parameters studied. Three of the apparatus have been discussed in detail previously and will be discussed only briefly in the following text. The fourth apparatus is new and will be described in detail. The apparatus are differentiated by three properties: the range of proton energies studied, the method of electron-energy analysis employed, and the type of gas target used. The data for 300 keV $\leq E_p \leq$ 1.5 MeV were taken at the Battelle, Pacific Northwest Laboratory (PNL), using a system that employs an electrostatic energy analyzer (EEA) for electrons ejected from a differentially pumped gas cell.[9] The EEA measurements were augmented at low electron energies by electron time-of-flight (TOF) measurements.[10] The TOF measurements give accurate relative cross sections for electrons ejected in collisions between protons and a gas beam for electron energies from 0.5 to 200 eV. For proton energies below 100 keV, the double-differential cross sections were mea-

sured with two independent EEA systems: one located at PNL and one at the University of Nebraska. The Nebraska system has been described by Rudd and Madison[11] (but slightly modified for this work). It uses a static gas target and a parallel-plate electrostatic analyzer. The PNL apparatus used for the low-energy proton work uses a cylindrical-mirror electrostatic analyzer to measure the electron yield from a proton-gas beam collision and is described below. The last two systems listed complement one another in the manner in which data are accumulated. The first can cover a wider range of angles, while the latter measures the electron energy distribution with a much finer energy grid.

Electrostatic analysis system for fast-proton collisions

The EEA system at PNL used for proton energies above 300 keV has been described in detail in Ref. 9. A proton beam from a Van de Graaff generator is magnetically analyzed and collimated. The transmitted beam passes through a differentially pumped gas cell and is collected in a Faraday cup. Electrons ejected from the cell by ion-atom collisions are energy analyzed in a cylindrical-mirror electrostatic analyzer and detected by a continuous-channel electron multiplier. Electron-energy spectra are obtained by applying a voltage to the analyzer that is controlled by an on-line computer. The number of transmitted electrons for a given number of protons ($\sim 10^{12}$) is stored, and the voltage stepped to the next value. When the analyzer voltage has been automatically stepped through the selected energy range, the ejection angles θ is changed manually and the next electron energy spectrum is taken. The resulting yields are converted to cross sections using the equation

$$\sigma(\epsilon, \theta) = \frac{N_e e^{\alpha P x}}{N_p P(dS)(\Delta E)(3.23\times 10^{16})} \text{ cm}^2/\text{eV sr atom}, \quad (1)$$

where N_e is the yield of electrons counted for an incident number of protons N_p; ΔE is the energy resolution of the cylindrical mirror; P is the target pressure in Torr; dS is the product of the solid angle subtended by the analyzer collimators and the proton path length observed within this solid angle; α is the electron absorption coefficient for the particular target gas and electron energy ϵ; and x is the effective path length of the electron through the target-gas density distribution.

Time-of-flight system

The electron time-of-flight system has been described by Toburen and Wilson.[10] The purpose for using this procedure is to provide relative electron-energy distributions that are reliable for very low energies of the ejected electrons. With this technique, the proton beam is pulsed by means of a high-voltage rf oscillator which sweeps the beam past a collimator. The proton pulses that pass through the collimator collide with a directed gas beam and are collected in a Faraday cup. The ejected electrons that pass through a collimation tube strike a channel electron multiplier which generates a timing pulse. The time between the proton-atom collisions and the electron pulse determines the energy of the electron. Time equal to zero is given by the position in the time spectrum of the photon peak (the electron multiplier being sensitive to short-wavelength light). Electron-energy spectra obtained from the time-of-flight distributions are reliable for electron energies from about 0.5 to 200 eV.

Electrostatic energy analysis for slow-proton collisions

Differentially pumped target

The EEA system used at the Behlen Laboratory has been recently described in a study of 5–100-keV proton collisions on helium.[11] In this system, an analyzed and collimated proton beam traverses a double-walled collision chamber and is collected in a Faraday cup. The inner chamber contains the target gas whose density is read by a capacitance manometer. The outer chamber provides for differential pumping of the electrostatic analyzer and the proton-beam input collimators. The system used in this study differs from that in Ref. 11 only in that a parallel-plate electrostatic energy analyzer was used with an energy resolution of 5.5%.

The measured electron yields were converted to cross sections by normalizing the present data to the measurements by Crooks and Rudd[5] at $E_p = 50$ keV and at each angle from 10° to 160°. Corrections made for electron absorption in the target gas, dead-time losses, geometrical factors, and similar effects may be found in Refs. 5 and 11. However, no preacceleration of the electrons was used, so the acceptance geometry could be accurately calculated.

Gas-beam target

The low-proton-energy EEA apparatus at PNL described in this section differs from that described in the previous section in detail. This apparatus uses a gas-beam target, a cylindrical-mirror analyzer, or time-of-flight energy analysis, and measures the electron energy distribution in a much finer energy grid.

The incident ion beam is produced in a rf ion

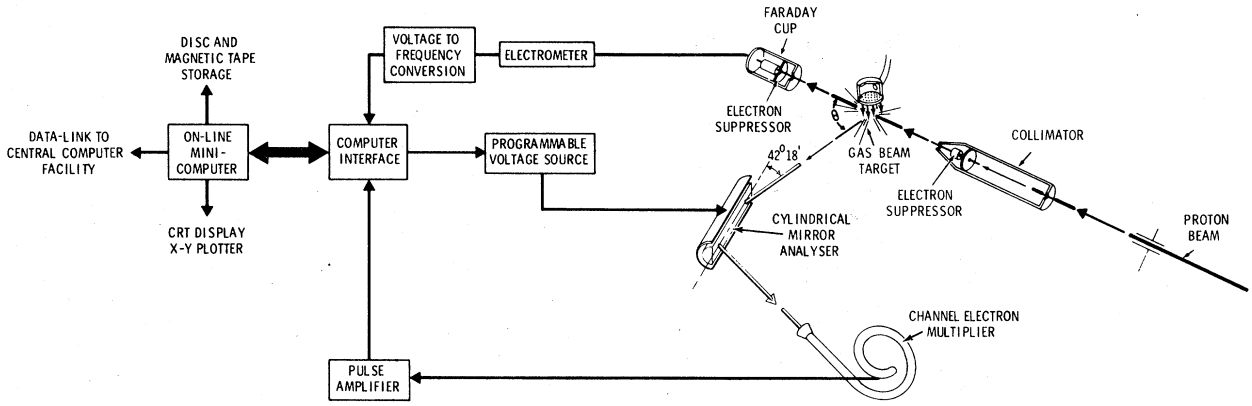

FIG. 1. Schematic diagram of the cylindrical-mirror electrostatic analyzer apparatus, gas-beam target, and associated apparatus used for the low-energy proton measurements at PNL.

source and accelerated through a potential generated by a 100-kV-transformer power supply. The beam is electrostatically focused and passes through horizontal and vertical deflection plates before entering the collision chamber. The deflection plates are gounded when a dc beam is used and are connected to a 1-MHz, 6-kV ellipse generator when a pulsed beam is needed. Following the deflection plates, the beam is magnetically analyzed and passes through a set of control slits, which provide a feedback signal that maintains energy control to with ±0.2%. The beam tube following the analyzing magnet was pumped to less than 10^{-6} Torr to minimize neutralization of the ion beam prior to entering the scattering chamber.

A schematic drawing of the apparatus is shown in Fig. 1. The analyzed proton beam enters the scattering chamber through the input collimators which include secondary electron suppression. The protons then pass through the molecular-gas beam and are collected in a Faraday cup that also has secondary electron suppression. The gas beam is formed by flowing the gas through a 100 : 1-aspect-ratio collimated hole structure (CHS). The gas pressure above the CHS is continuously monitored by a capacitance manometer and is automatically controlled by a servo-driven valve to within ±1%. The gas-beam density corresponds to a static gas pressure of approximately 1×10^{-4} Torr, whereas the background chamber pressure is 3×10^{-7} Torr.

Stray magnetic fields are reduced by housing the collision chamber in an 80-cm-o.d. double-walled magnetic shield. This shield and a set of external Helmholz coils reduce the magnetic fields in the collision region to less than 5 mG. Stray electric fields are reduced by coating exposed interior surfaces of the chamber with colloidal graphite.

The energy of the electrons ejected in the ion-gas collisions is measured using the cylindrical-mirror EEA that has been described earlier.[9] The electrons transmitted through the EEA are detected by a continuous-channel electron multiplier. The voltage applied to the EEA is controlled by an on-line computer that steps the analyzer voltage after a preset charge has been collected in the Faraday cup. The details of the programmable voltage supply are described by Ratcliffe.[12]

Owing to the lack of detailed knowledge concerning the target-gas density distributions in the gas beam, the measured electron yields cannot be directly converted to cross sections. This necessitates a second set of EEA measurements for each target gas for proton energies where there are well-known cross-section data. To make this comparison, the scattering chamber is moved to the laboratory's 2-MV Van de Graaff accelerator and ejected-electron yields are measured at 1-MeV proton energy for the same target-gas pressure used in the low-energy measurements, and the results are compared to the absolute measurements previously made using a differentially pumped gas cell (see Ref. 9 for a description of this latter system). This normalization procedure is the largest source of systematic error since it compounds the errors involved in both the absolute measurement and the calibration measurement.

The transmission of the EEA decreases below about 20-eV electron energy due to stray fields within the analyzer. The transmission may be improved by preaccelerating the incoming electrons. The difficulty with using preacceleration is that a lens may be formed by the input collimators which can change the acceptance solid angle of the analyzer. In order to check the validity of the preacceleration technique, the yield of ejected electrons

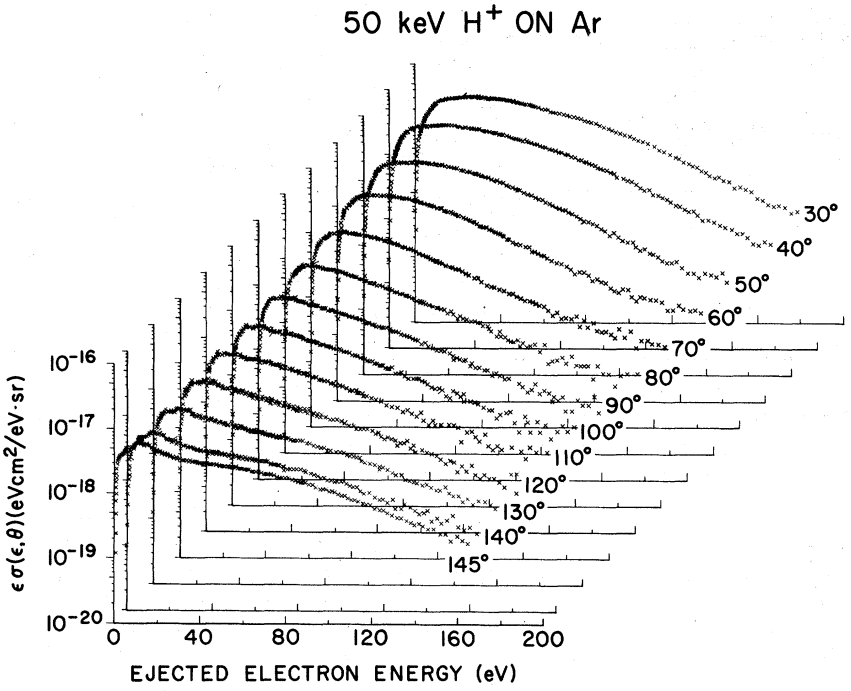

FIG. 2. Cross sections, differential in electron energy ϵ and emission angle θ, for ejection of electrons by 50-keV protons on Ar.

was measured for incident 50-keV H^+ using an independent time-of-flight (TOF) technique whose relative transmission from 1.0 to 200 eV is known to be constant.[10] A pulsed proton beam is produced by a 1-MHz chopper that is 2.0 m upstream of the input collimators. A time difference is then measured between the zero crossover of the chopper and when the ejected electrons arrive at the channel electron multiplier. Just before entering the detector, the electrons are accelerated through 50 eV in order to assure detection. This additional velocity was accounted for in converting the time spectrum to an energy spectrum. Time equal to zero and time resolution are derived from the position and width of the peak associated with deexcitation of the target via photon emission. The time resolution was 7.5 nsec. The TOF measured yields were then normalized to the EEA yields in the electron energy range from 20 to 200 eV. The EEA yields agreed well with the TOF yields down to 10 eV when no preacceleration was used and were in good agreement with TOF yields to 1 eV when 10-V preacceleration was used.

The error limits assigned to the data obtained from the differentially pumped system and the static gas system have been reviewed elsewhere.[13] For $\epsilon \geq 20$ eV, the estimated uncertainty in the absolute cross sections is ±20%. The data from the gas-beam system were normalized to the differentially pumped system and are susceptible to further statistical errors. The limits on the accuracy of these latter measurements are ±25% for $5 \leq \epsilon \leq 100$ eV.

RESULTS

The general features of the electron-ejection spectra are shown in Fig. 2 for 50-keV protons on argon. These data are taken using the low-energy EEA system at PNL. Note that the data are plotted as electron energy times ejection cross section so that the number of decades necessary to display the data is reduced. As plotted, the distributions peak at about 10 eV at forward ejection angles and decreases with increasing electron energy ϵ and with increasing ejection angle over the range shown. The autoionization lines of Ar are noticeable at electron energies below 16 eV, particularly in the back angles. In Fig. 3, the autoionization lines are observed to contribute a large fraction of the ejected-electron spectra for lower projectile energies. The Behlen EEA data are also shown. For $E_p = 50$ keV, the PNL and Behlen data agree within experimental error down to 2 eV. At 5 keV, the two measurements are in good agreement down to 4 eV. At this low proton energy, the contribution due to autoionization is large. A small error made in measuring the electron energy may affect the measured yield by as much as a factor of 2. As noted by Rudd and Macek,[13] the electron-energy spectra may be shifted by using so high a beam current that space-charge effects change the po-

tential difference between the target region and the analyzer. However, this should lead to noticeable errors only for low E_p, where the autoionization component is large. Since the beam currents obtainable at low E_p are relatively small (for $E_p = 5$ keV, one typically has less than 50 nA through the 1-mm apertures), the effect is expected to be negligible.

The angular distributions of the double-differential cross sections are shown in Fig. 4 for $\epsilon = 10$ and 20 eV. Where overlap occurs between results from PNL and Behlen Laboratory, the agreement is good. Slight disagreement exists for 5-keV proton bombardment, but the statistics are also poorest there. From 300 keV to 1.5 MeV, the broad maxima due to binary-encounter collisions are visible at intermediate angles. This effect has disappeared by $E_p = 50$ keV, and the distributions have become quite anisotropic. The maximum in the cross sections is now in the forward direction with a smaller local maximum in the backward direction. As E_p decreases further, the distributions again become more isotropic and are nearly flat by $E_p = 5$ keV and $\epsilon = 10$ eV.

The energy distributions shown in Fig. 5 were obtained by integrating the double-differential cross sections (DDCS) over angle. For $E_p \leq 300$ keV, the Behlen data were used since it covers a wider angular range. For $E_p \geq 300$ keV, the PNL data were used. For low-energy protons, the cross sections tend toward the same value of 2.6×10^{-17} cm^2/eV as ϵ approaches 2 eV. For H^+ on He, this value was found to be 9×10^{-18} cm^2/eV.[11] This low-energy cross section seems to scale

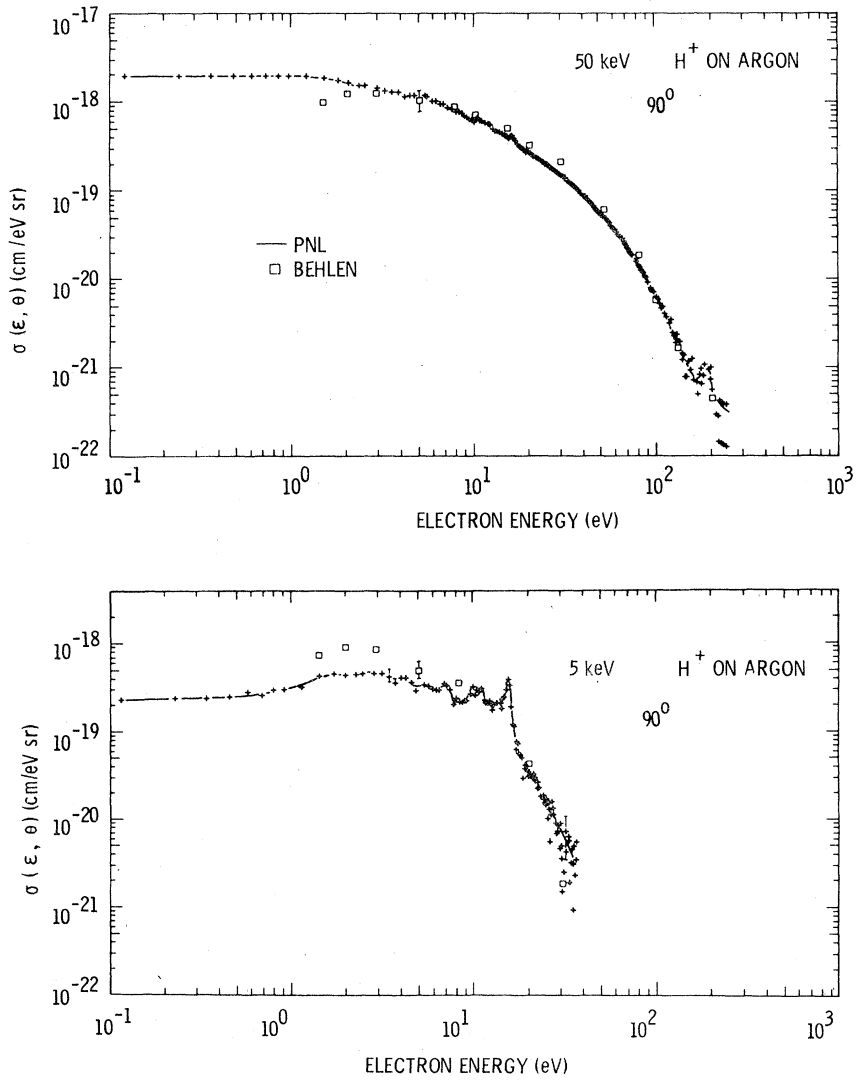

FIG. 3. Energy distribution of electrons ejected at 90° by 50- and 5-keV protons on Ar: PNL(+) and Behlen (●). The lines are due to the autoionization of Ar.

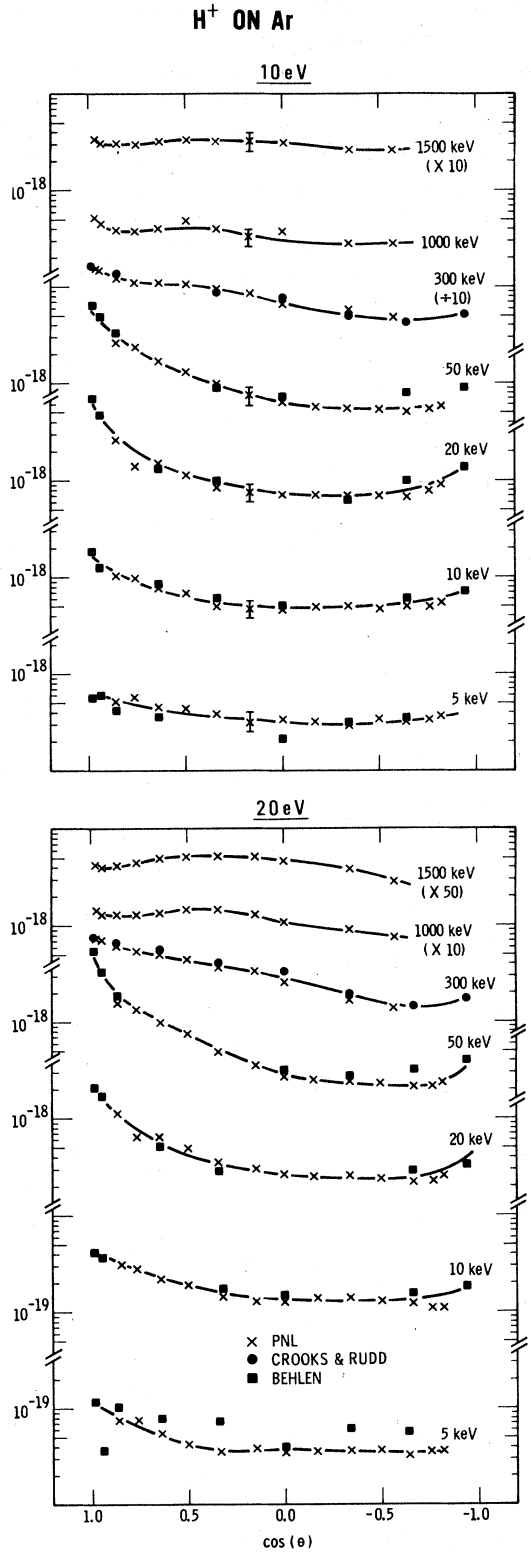

FIG. 4. Angular distributions of the double-differential cross sections for 10- and 20-eV electrons: PNL (×), Behlen (■), and Crooks and Rudd (Ref. 5) (●).

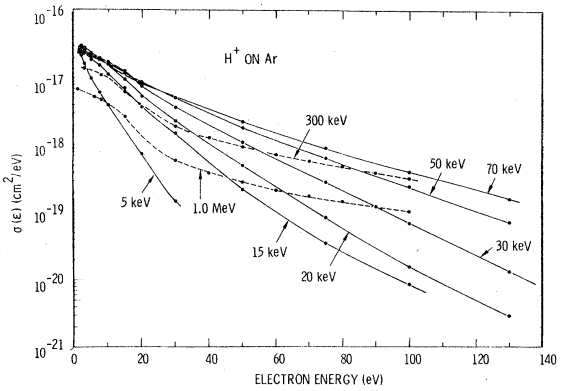

FIG. 5. Electron-energy distributions integrated over angle.

roughly as the number of loosely bound electrons (e.g., two for He and eight for Ar). For the fast protons ($E_p \geq 300$ keV), the scaling breaks down and the zero-energy electron cross section becomes a function of the proton energy.

A further check on the consistency of the data is provided by integration of the DDCS over electron energy and ejection angle and comparison of the results to measured total ionization cross sections. A comparison of results obtained from integration of our measured differential cross sections to several previously reported ionization cross sections for proton- and electron-impact ionization of argon is shown in Fig. 6. Integration of the DDCS over ϵ and θ at $E_p = 1.5$ MeV give a total ionization cross section $\sigma_I = 0.99 \times 10^{-16}$ cm^2,

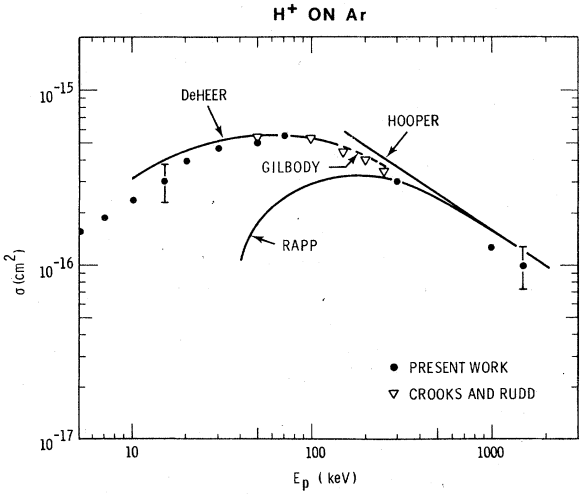

FIG. 6. Total ionization of argon by protons and electrons. Protons: ●, present work; ▽, Crooks and Rudd (Ref. 5), De Heer *et al.* (Ref. 17), Gilbody and Lee (Ref. 15), Hooper *et al.* (Ref. 14). Electrons: Rapp and Englander-Golden (Ref. 16).

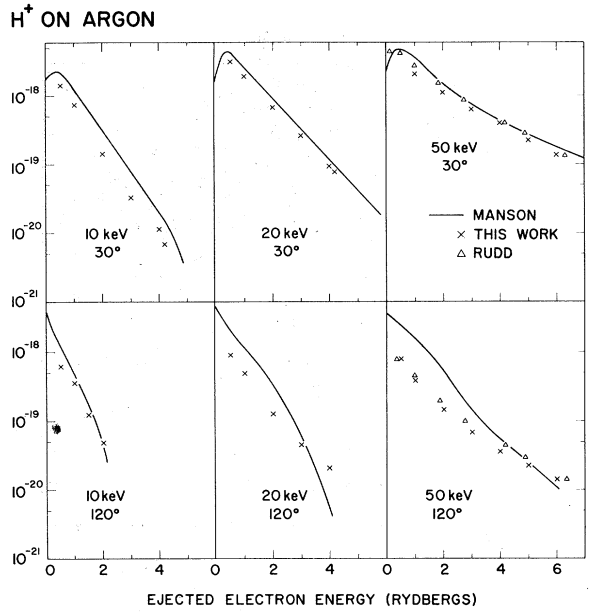

FIG. 7. A comparison of the PNL low-energy proton data (×) to the data of Crooks and Rudd (Ref. 5) (Δ) and the PWBA calculation of Manson (Ref. 4) (solid line).

and at $E_p = 1.0$ MeV, $\sigma_I = 1.24 \times 10^{-16}$ cm^2; both are 25% below the values given by Hooper *et al.*[14] At $E_p = 300$ keV, our measurements give a total ionization cross section $\sigma_I = 3.08 \pm 0.50 \times 10^{-16}$ cm^2, which is 16% lower than the data of Hooper *et al.*,[14] 12% below an extrapolated value from Gilbody and Lee,[15] and agrees with the 163-eV (i.e., equal velocity) electron-impact data of Rapp and Englander-Golden.[16] At 50 keV, our value is $5.05 \pm 1.50 \times 10^{-16}$ cm^2, which is 10% below those of Gilbody and Lee[15] and De Heer *et al.*[17] At 10 keV, we get $2.34 \pm 0.70 \times 10^{-16}$ cm^2, which is 27% below that of De Heer *et al.*[17] and 19% below that of Gilbody and Lee.[15]

Figure 7 presents a comparison of the PNL low-energy proton data and the data of Crooks and Rudd[5] to the PWBA theory of Manson *et al.*[4] The calculation of Manson *et al.* uses Hartree-Slater initial discrete- and final continuum-state wave functions for the electrons making all transitions except the $3p$-ϵd. For this transition, Manson used a full continuum Hartree-Fock calculation as has been shown to be necessary from optical data.[2,3] The $2s$, $2p$, $3s$, and $3p$ subshells were included in the calculation, and the partial cross sections summed to provide the results shown in Fig. 7. The calculated cross sections, shown as a solid line, agree with the experimental data best in the forward direction. At 50 keV and 30° ejection angle, theory and experiment are essentially identical. As E_p decreases, theory increasingly overestimates the cross section, but continues to describe the shape quite well. The agreement in the backward direction is not as good, either in magnitude or shape. Changes in curvature, particularly noticeable between 10 and 20 keV at 120°, are not correctly predicted.

The choice of wave functions can have appreciable effects on the claculated cross sections. In Fig. 8, we compare the measured DDCS to the theories of Manson *et al.*[4] and Madison.[8] Madison's calculation differs substantially from that of Man-

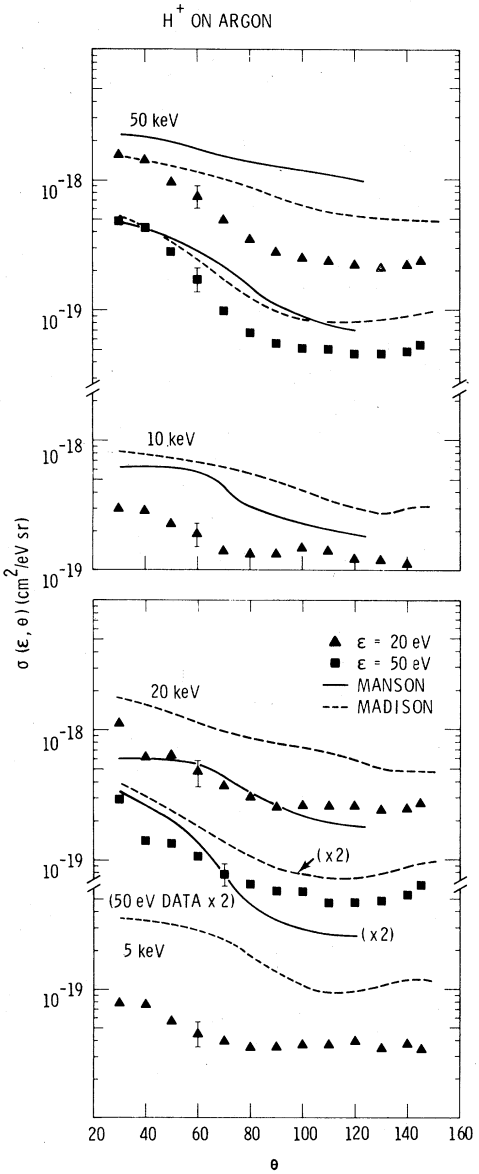

FIG. 8. Comparison of the present data at 20 eV (▲) and 50 eV (■) to the PWBA calculation using Hartree-Fock wave functions (solid lines) and to the PWBA calculation using Hartree-Slater wave functions (dashed lines).

son *et al.* only in that it used Hartree-Slater wave functions throughout. Thus, in the following paragraphs, the Manson *et al.* calculations will be labeled HF and those of Madison HS. The curve labeled "Manson" in Fig. 8 was derived graphically from a set of 12 curves like the ones shown in Fig. 7. Thus, the shape of the HF curves may not be precise but are representative.

The comparison between HF and HS predictions relative to the experimental data in Fig. 8 does not show either theory to be consistently closer to the experiment. Both do relatively better in the forward direction than in the backward direction and better as a whole for the higher electron energies. The HS values are generally more isotropic than experiment and increasingly overestimate the cross sections as E_p decreases. The HF values show no clear systematics regarding agreement with experiment as a function of E_p. At $E_p = 50$ keV, HF fits the $\epsilon = 50$ eV experimental points better than the 20-eV points. This reverses at $E_p = 20$ keV, where HF is closer for $\epsilon = 20$ eV rather than $\epsilon = 50$ eV. Then, by $E_p = 10$ keV, HF is a factor of 2 above the experimental value.

The anticipated improvement of the HF results over the HS is not realized for low E_p. There are two reasons for this to be the case: one physical, the other computational. In a collision between a proton with energy E_p and a bound electron, if the electron is ejected with energy ϵ, then by conservation of energy and momentum, the minimum momentum transfer to the bound electron is given by[18,19]

$$(Ka_0)^2_{\min} = (\epsilon + I)^2/4TR\,,$$

where T is $E_p/1836$, I is the ionization potential, a_0 is the Bohr radius, and R is the Rydberg energy. This minimum momentum transfer appears as the lower limit of an integral in the PWBA. The upper limit is approximately $4T/R$. However, since the integrand falls off rapidly,[19] the integration is cut off at some arbitrary value $(Ka_0)^2_{\max}$, where the integrand is sufficiently small. For 1-MeV protons on argon ejecting 60-eV electrons, $(Ka_0)^2_{\min} = 0.2$. For 20-keV protons on argon ejecting 10-eV electrons, $(Ka_0)^2_{\min} = 1.1$. Experience has shown that the integrands in the integral over momentum transfer differ between the HF and HS primarily at the optical limit.[4,18,20] For low E_p, this limit in momentum transfer is not reached, and the two formulations should give much the same results. That the curves differ in Fig. 8 is probably due to differences between the numerical methods used in the two calculations. The HS matrix elements are computed for a fixed number of values of K between $K_{\min}$ and $K_{\max}$. The HF matrix

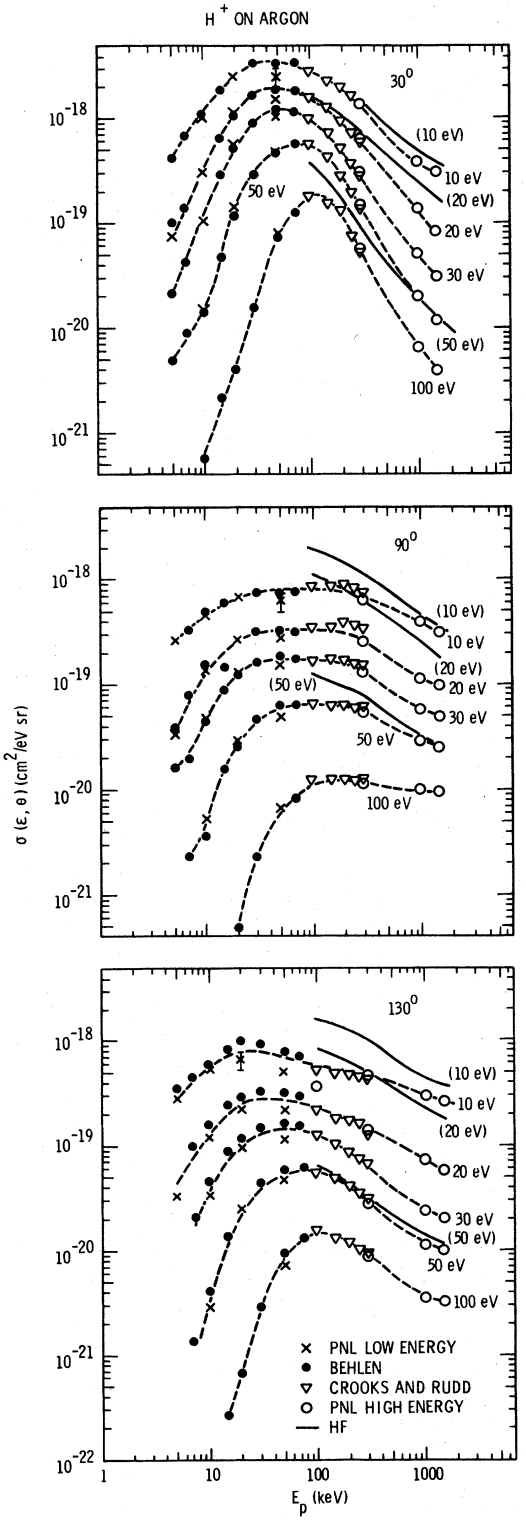

FIG. 9. Double-differential cross sections as a function of proton energy E_p: PNL low-energy apparatus (×), Behlen (●), Crooks and Rudd (Ref. 5) (▽), PNL high-energy apparatus (○), and the PWBA calculation of Manson (Ref. 4) (solid lines).

elements are computed for a fixed set of values for K. The mesh of points used in the integrations may be denser for the HS than for the HF, particularly at low E_p. Thus, at low E_p, the HS might give the more accurate representation of the PWBA.

Figure 9 displays the DDCS at five electron energies from 10 to 100 eV, at three ejection angles, and over the full range of proton energies studied. The present data are compared to that of Crooks and Rudd[5] and the PWBA theory of Manson *et al.*[4] The agreement between the data of PNL, Behlen Laboratory, and Crooks and Rudd is seen to be good for all proton and electron energies and electron-ejection angles. The somewhat larger differences at $E_p = 50$ keV and $\epsilon = 10$ and 20 eV, and $\theta = 30°$ and 130° have not been fully explained. It is possible that a neutral hydrogen component in the incident proton beam, arising from charge transfer with the residual gas in the beam line, could cause such a discrepancy. By raising the pressure to 5×10^{-5} Torr in the beam line after the analyzing magnet on the PNL system, thus increasing the neutral component of the incident beam, the Behlen results could be duplicated. However, for this effect to cause the disparities, it would require that only occasional runs with the Behlen system had been similarly affected. This is not thought to be the case and the cause of the difference remains unexplained. The agreement between the HF results shown for 100 keV $\leq E_p \leq$ 1.5 MeV and measured cross sections is generally better for the higher-energy ejected electrons. The failure of the calculation for $\epsilon < 50$ eV has been discussed earlier and has been attributed to the inability of the HF Born calculation to predict accurately the position of the Cooper minimum in argon.[1]

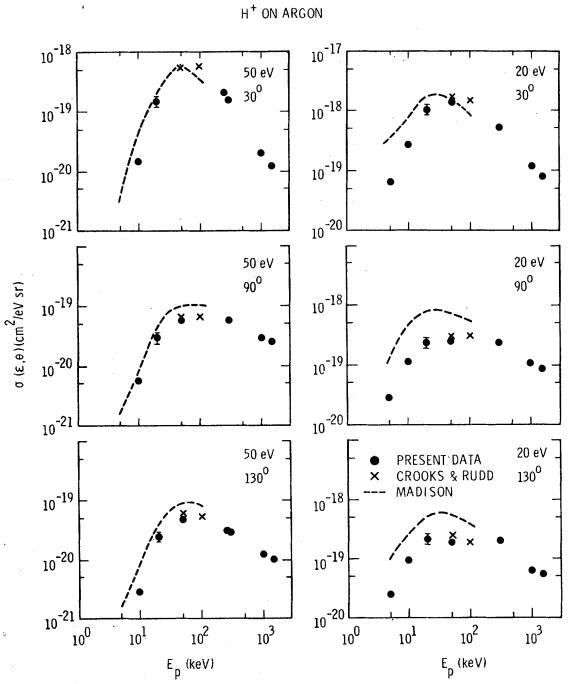

FIG. 10. Double-differential cross sections as a function of proton energy E_p: present data (●), Crooks and Rudd (Ref. 5) (×), and the PWBA calculations of Madison (dashed line).

In Fig. 10 is shown a comparison of the measured cross sections to those calculated using HS wave functions and the Born approximation. This comparison for two representative electron energies and three ejection angles illustrates the low energy dependence of these cross sections. The calculations are nearest to agreement for the higher-energy electrons ejected in the forward direction. The shape of the distributions are more nearly represented for ejection of the higher-energy electrons, whereas even the peak in the distribution is improperly given by the calculation for 20-eV electrons.

CONCLUSIONS

We have measured electron-ejection cross sections differential in electron energy and ejection angle for protons incident on Ar-gas targets over the proton energy range E_p from 5 keV to 1.5 MeV. The measurements are believed accurate to within ±20% for electron energies greater than 1 eV for $E_p > 50$ keV where the additional time-of-flight analysis was used and for electron energies greater than 5 eV for $E_p < 50$ keV. The agreement between the present data and that of Crooks and Rudd[5] at $E_p = 50$ and 250 keV is within experimental error. The total ionization cross sections obtained by integration of the DDCS agreed to within experimental error with the results of direct measurements.

The present data for $E_p < 100$ keV were compared to two PWBA calculations that used slightly different wave functions. The PWBA calculation by Madison (HS) used Hartree-Slater wave functions for all initial discrete and final continuum states. The PWBA calculation by Manson (HF) used Hartree-Slater wave functions for all channels except the $3p$-ϵd, where full continuum Hartree-Fock wave functions were used, a modification shown to be necessary through photoionization measurements. It was found that both the HF and HS values increasingly overestimated the cross sections as E_p decreased below 50 keV. As the proton energy is increased, the HF calculations provide double-differential cross sections in close agreement with experiment for ejected-electron energies above approximately 50 eV. For the low proton energies,

the HF calculation, however, displays no marked or consistent improvement over the HS. The discrepancies between the PWBA results and experiment are probably due to the increasing relative importance of molecular promotion and autoionization channels as the number of channels open to direct ionization decreases with decreasing proton energy.

ACKNOWLEDGMENTS

The authors gratefully acknowledge the help of W. E. Wilson for the development of systems software and C. A. Ratcliffe for the development of systems interfacing. We also wish to thank S. T. Manson and D. H. Madison for providing the theoretical results used in the text.

---

*This paper is based on work performed under United States Energy Research and Development Agency Contract No. EY-76-C-06-1830, National Science Foundation Grant No. GP-40, 353, and Battelle Institute Contract No. 2322245063.

[1]S. T. Manson and L. H. Toburen, in *The Physics of Electronic and Atomic Collisions*, edited by J. S. Risely and R. Begalle (University of Washington Press, Seattle, 1975), p. 751.
[2]A. E. Starace, Phys. Rev. A 3, 1242 (1971).
[3]D. J. Kennedy and S. T. Manson, Phys. Rev. A 5, 227 (1972).
[4]S. T. Manson, L. H. Toburen, D. H. Madison, and N. Stolterfoht, Phys. Rev. A 12, 60 (1975).
[5]J. B. Crooks and M. E. Rudd, Phys. Rev. A 3, 1628 (1971).
[6]H. Gabler, thesis (Hahn-Meitner-Institut für Kernforshung, Berlin, 1974) (unpublished).
[7]M. E. Rudd, Radiat. Res. 64, 153 (1975).
[8]D. H. Madison, Phys. Rev. A 8, 2449 (1973).
[9]L. H. Toburen, Phys. Rev. A 3, 216 (1971).
[10]L. H. Toburen and W. E. Wilson, Rev Sci. Instrum. 46, 852 (1975)
[11]M. E. Rudd and D. H. Madison, Phys. Rev. A 14, 128 (1976).
[12]C. A. Ratcliffe, Rev. Sci. Instrum. 46, 1586 (1975).
[13]M. E. Rudd and J. H. Macek, Case Stud. At. Phys. 3, 47 (1972).
[14]J. W. Hooper, D. S. Harmer, D. W. Martin, and E. W. McDaniel, Phys. Rev. 125, 2000 (1962).
[15]H. B. Gilbody and A. R. Lee, Proc. R. Soc. A 274, 364 (1963).
[16]D. Rapp and P. Englander-Golden, J. Chem. Phys. 43, 1464 (1965).
[17]F. J. De Heer, J. Schutten, and H. Moustafa, Physica (Utr.) 32, 1766 (1966).
[18]S.T. Manson, Phys. Rev. A 6, 1013 (1972).
[19]M. Inokuti, Rev. Mod. Phys. 43, 297 (1971).
[20]David J. Kennedy and Steven Trent Manson, Phys. Rev. A 5, 227 (1972).